

Published in final edited form as:

Acta Biomater. 2013 March ; 9(3): 5771–5779. doi:10.1016/j.actbio.2012.10.043.

Surface Properties and Ion Release from Fluoride-Containing Bioactive Glasses Promote Osteoblast Differentiation and Mineralisation *in vitro*

E. Gentleman^{1,2,4,*}, M.M. Stevens^{1,2,3}, R.G. Hill⁵, and D.S. Brauer^{5,6,*}

¹Department of Materials, Imperial College London, London SW7 2AZ, UK

²Institute of Biomedical Engineering, Imperial College London, London SW7 2AZ, UK

³Department of Bioengineering, Imperial College London, London SW7 2AZ, UK

⁴Craniofacial Development & Stem Cell Biology, King's College London, London SE1 9RT, UK

⁵Department of Materials, Queen Mary University of London, London E1 4NS, UK

⁶Otto Schott-Institut, Friedrich-Schiller-Universität, Jena, Germany

Introduction

Bioactive glasses (BG) have the ability to bond directly with living tissue *via* the formation of a hydroxycarbonate apatite-like layer on their surface, and are therefore utilised in a variety of dental and orthopaedic applications [1, 2]. However, this is not their only mechanism of action. BG can also be designed to release ions that stimulate specific cell behaviour. Indeed, we have recently reported on BG that release strontium ions, the active component of the osteoporosis drug strontium ranelate, which act to both promote osteoblast activity and inhibit osteoclast activity [3].

Fluoride is widely recognised for its ability to prevent dental caries as it inhibits dentine and enamel demineralisation [4], however, it also affects the axial skeleton. That is, clinical examinations of osteoporotic patients have demonstrated that fluoride treatment stimulates bone formation [5]. Nevertheless, in placebo-controlled, double-blind clinical trials, sodium fluoride (NaF) was found not to be efficacious in preventing osteoporosis-related fractures [6, 7]. In subsequent detailed analyses of these trials, fluoride's lack of efficacy was attributed to its substitution into bone apatite, creating structurally and mechanically inferior bone, as mineral crystal size and crystallinity increased [8]. Consequently, fluoride's use as an osteoporosis treatment was largely dismissed. Moreover, this seemed judicious as osteomalacia was reported in patients treated with NaF [9], and skeletal fluorosis, which is endemic in areas with high levels of fluoride in the ground water, is known to cause a range of skeletal abnormalities [10].

*To whom all correspondence should be addressed: Dr. Eileen Gentleman, Craniofacial Development and Stem Cell Biology, CFD19, Floor 27, Tower Wing, Guy's Hospital, Dental Institute, King's College London, London SE1 9RT, UK, +44 (0) 20 7188 7388, eileen.gentleman@kcl.ac.uk and Prof. Dr. Delia S. Brauer, Otto-Schott-Institut, Friedrich-Schiller-Universität, Fraunhoferstr. 6, 07743 Jena, Germany, +49 3641 948510, delia.brauer@uni-jena.de.

As clinical trials with fluoride failed to demonstrate clear anti-fracture efficacy, other osteoporosis drugs have come into favour. Anti-catabolic agents such as bisphosphonates, which block osteoclast-mediated bone resorption *via* inhibition of the mevalonate pathway [11] are widely prescribed. However, anti-catabolic agents only prevent further bone resorption and do not promote bone formation. Furthermore, long-term bisphosphonate use has been associated with osteonecrosis of the jaw [12] and atypical, low-energy femur fractures [13], which has created reluctance among some clinicians to prescribe them. Anabolic agents such as recombinant parathyroid hormone (PTH), which stimulate osteoblast-mediated bone matrix formation [14], are also often administered. However, PTH is expensive and requires daily subcutaneous injections. As a result, alternative treatments, such as inexpensive NaF, have recently been re-examined [15].

In vitro studies point towards a small dosing range for NaF that will successfully promote osteoblast activity [16], and recent meta-analyses have shown that fluoride is efficacious in preventing osteoporosis-related fractures when administered at doses lower than those used in the widely reported clinical trials [17]. Furthermore, *in vitro* studies have demonstrated that fluoride has an anabolic effect on bone, enhancing osteoblast proliferation [18, 19] and alkaline phosphatase activity [19–21]. The effect, however, seems to be strongest on osteoblast precursors as opposed to mature cells [22, 23], suggesting that fluoride may promote osteoblast differentiation or maturation. Moreover, cells isolated from animals administered fluoride *in vivo* showed higher proliferative potential than those isolated and subsequently treated *in vitro* [24]. Taken together, these data suggest the importance of the timing of the administration of fluoride, and support a role for short-term treatment of less mature cells as a route for gaining the greatest benefit. Therefore, therapies such as BG that have the potential to locally administer therapeutic doses of fluoride over a predictable time frame, may be useful for stimulating new bone formation.

One important factor in designing BG is network connectivity (NC), a measure of the number of bridging oxygen atoms per network forming element, and an indicator of BG solubility, reactivity and bioactivity [25]. Here, by holding the ratio of network former to network modifier constant whilst adding CaF₂, we created a BG series with increasing amounts of fluoride, but with constant NC (assuming fluoride only associates with calcium, *i.e.* Si-F bonds are not formed [26]). This allowed us to examine the effects of fluoride in BG on human osteoblast cells *in vitro* without complications caused by changes in the silicate network structure. We also separated the effects of ions released from BG from the effects elicited by cells' complex interactions with the apatite-forming BG surface and examined how both factors influenced human osteoblast activity.

Materials and Methods

Preparation of BG discs

BG in the system SiO₂–P₂O₅–CaO–Na₂O were prepared by a melt–quench route. CaF₂ was added whilst NC and the ratio of all other components were kept constant (Table 1). Mixtures of analytical grade SiO₂ (Prince Minerals Ltd., Stoke-on-Trent, UK), P₂O₅, CaCO₃, Na₂CO₃ and CaF₂ (all Sigma-Aldrich, Gillingham, UK) were melted in a platinum–rhodium crucible for 1 h at 1430°C. A batch size of 100 g was used. After melting, BG were

rapidly quenched in deionised water (dH₂O) to prevent crystallisation. BG rods were produced by casting the melt into pre-heated graphite moulds (10 mm diameter) and subsequently annealing at the glass transition temperature, which varied between 514 and 439°C [27]. Rods were sectioned into 1 mm thick discs on a low-speed diamond saw (IsoMet[®], Buehler GmbH, Düsseldorf, Germany) using isopropanol as a coolant. Prior to cell culture experiments, BG discs were sterilised under UV light for 2 h on each side and pre-conditioned in 1 mL of culture medium (RPMI 1640 with 1X penicillin/streptomycin solution; Invitrogen, Paisley, UK) for 4 days. Cell culture medium was exchanged daily and stored at -20 °C.

Elemental analysis of ions released from BG

Culture medium samples were diluted by a factor of 10 in dH₂O, and concentrations of calcium and silicon were measured on an inductively coupled plasma – optical emission spectrometer (ICP-OES) (iCAP 6000, Thermo Scientific, Waltham, MA, USA). Fluoride concentration was measured using a fluoride-selective electrode (Orion 9609BNWP with Orion pH/ISE meter 710; Thermo Scientific). Calibration was performed using standard solutions prepared using either dH₂O or tris buffer for ICP-OES and fluoride measurements, respectively.

Cell culture with BG discs

The human osteosarcoma cell line, Saos-2, was obtained from the European Collection of Cell Cultures (Salisbury, UK) and cultured under standard conditions (37 °C, 5% CO₂/95% air, 100% humidity) in RPMI 1640 with 10% (v/v) foetal bovine serum (FBS) and 2 mM L-glutamine (all from Invitrogen). One BG disc per well was seeded at 30,000 cells/cm². The surrounding tissue culture plastic was likewise seeded at 30,000 cells/cm² to assess both the effects of culture in contact with the BG and that resulting from exposure to their dissolution products, as previously described [28]. The culture medium was exchanged 3 times per week and stored at -20 °C. Discs were moved to fresh wells prior to assays to allow separate analyses of cells cultured in contact with discs from those only exposed to their dissolution products.

For experiments with NaF, 30,000 cells/cm² were seeded in 96-well plates and cultured for up to 28 days in medium as above supplemented with 100 µM NaF (Sigma) for the indicated time period. Otherwise cells received standard culture medium, which was exchanged 3 times per week.

X-ray diffraction (XRD) of BG surfaces

After 7, 14, or 28 days of culture, cells were removed and BG discs were rinsed in dH₂O and air dried. Surfaces were then examined by XRD (X'Pert PRO MPD, PANalytical, Cambridge, UK; 40 kV/40 mA, CuKα, collected at room temperature) and analysed using X'Pert HighScore Plus software (v2.0, PANalytical, The Netherlands) and the International Centre for Diffraction Data database. Diffraction patterns were compared to reference patterns of hydroxycarbonate apatite (JCPDS 19-272) and fluorapatite (JCPDS 31-267).

Scanning electron microscopy (SEM) to visualise cells and BG apatite formation

After 7, 14 and 28 days in culture, some BG discs were rinsed with phosphate buffered saline (PBS) and fixed for 40 minutes in 2.5% (w/v) glutaraldehyde in sodium cacodylate buffer (pH 7.3) at 4 °C. Discs were then rinsed with PBS, dehydrated in a graded ethanol series, incubated with hexamethylsilasane (Sigma), sputter coated with gold and viewed on an FEI Inspect F SEM (FEI, Eindhoven, Netherlands) using the secondary electron mode at 10 kV. Other BG discs used for cell culture analyses and XRD were also analysed by SEM to visualise apatite formation. Discs were sputter coating with gold/palladium and viewed in an SEM as above.

Cell viability staining on BG discs

Cell viability on BG discs was visualised after 14 and 28 days in culture by staining adherent cells using a Live/Dead[®] kit (Invitrogen). Live/Dead[®] utilises Calcein AM, which fluoresces green upon enzymatic conversion to calcein in live cells, and Ethidium Homodimer-1, which is excluded from live cells, but binds to nucleic acids in dead cells producing a red fluorescence. Cell-seeded BG discs were rinsed with PBS and transferred to a solution containing 1 µM Calcein AM and 1 µM Ethidium Homodimer-1 in PBS and incubated for 30 minutes, as previously described [29]. Cells were visualised under epifluorescent light and representative images were taken.

Total cell quantification of cells cultured with BG

The total number of cells attached to BG discs and in tissue culture plastic wells was determined by quantifying the activity of the ubiquitous cytosol enzyme, lactate dehydrogenase, using a CytoTox 96[®] Non-Radioactive Cytotoxicity Assay (Promega, Southampton, UK) as previously described [30, 31]. Briefly, cells were lysed in a 0.9% (v/v) solution of Triton X-100 (Sigma) in dH₂O. The resulting lysate was then reacted with the kit's substrate solution for 30 minutes. The reaction was stopped with the addition of 1M acetic acid and the resulting product was measured on a colorimetric plate reader at 490 nm.

Alkaline phosphatase (ALP) activity in cells cultured with BG

ALP activity was measured by colorimetrically quantifying ALP's conversion of p-nitrophenyl phosphate to p-nitrophenyl. At indicated time points, cultures were lysed in 0.9% (v/v) Triton X-100 in dH₂O and reacted with a solution of 1 mg/mL p-nitrophenyl phosphate in 0.1 M glycine buffer with 0.1 mM ZnCl₂ and 0.1 mM MgCl₂ (pH = 10.4; all from Sigma). The reaction was stopped by adding 1 M NaOH and absorbance at 405 nm was measured on a colorimetric plate reader.

AlamarBlue activity in cells treated with NaF

AlamarBlue[®] (Invitrogen) activity, a measure of cell metabolic activity, was quantified in Saos-2 treated with NaF after 7, 14 and 28 days in culture according to the manufacturer's instructions. Briefly, substrate solution was added to culture medium on live cells to create a 10% (v/v) solution and incubated for 1 h. The medium was then removed to an opaque 96-well plate and fluorescence was quantified at 560 nm excitation/590 nm emission.

Total protein quantification to normalise ALP activity in cells treated with NaF

ALP activity in NaF treated cultures was normalised to total protein content per well, which was determined using a BCA protein assay kit (Pierce, Thermo Scientific, UK) according to the manufacturer's instructions.

Interleukin-6 (IL-6) release from cells cultured with BG discs

Release of IL-6 by Saos-2 cultured with BG discs for 7 and 14 days was quantified with a human IL-6 ELISA kit (R&D Systems, Abingdon, UK) according to the manufacturer's instructions.

Statistical analyses

Cell assay data from BG disc cultures are presented as means \pm standard deviations and represent data from 8 individual discs. Assays on NaF-treated cultures are also presented as means \pm standard deviations and represent 5 independent experiments with 6 replicates per experiment. The IL-6 ELISA was conducted with 3 samples per condition. Comparisons of BG assay data were made using a one-way ANOVA with post-hoc Tukey test; NaF treatment results were compared with one-way ANOVA and post-hoc LSD test. Significance is indicated when $p < 0.05$. Elemental analysis was carried out with at least 3 samples per condition. Fluoride concentration was determined from 3 samples per condition with the exception of at days 14 and 28 when low fluoride concentrations near the detection limit of the instrument rendered replicates superfluous.

Results

BG formation

BG rods and discs were optically clear. Solid state nuclear magnetic resonance (NMR) spectroscopy previously demonstrated that BG silicate structure, consisting predominantly of Q^2 chains, remained constant when adding CaF_2 [26].

Elemental analysis of ions released from BG

The concentration of calcium in cell culture medium increased from its baseline of approximately 24 ppm to between 31 and 45 ppm after 2 days culture with all BG compositions (Table 2). Calcium concentration in all groups remained higher than baseline for the entire 28-day culture period with the exception of the 13.62 and 17.76 mol% CaF_2 groups, for which calcium concentration was lower than baseline after 14 and 28 days in culture. Silicon release into cell culture media varied depending on BG composition. BG with 0 mol% CaF_2 continued to release silicon at levels between \sim 20 and 50 ppm throughout the culture period. In contrast, by later time points, the 13.62 and 17.76 mol% CaF_2 groups released little to no silicon.

Fluoride release was dependent on fluoride concentration in BG, as compositions with higher fluoride contents gave higher fluoride concentrations in the culture medium (Table 3). The majority of fluoride, however, was released during the pre-conditioning period and the first week in culture. Indeed, after 14 days incubation of the BGs in culture medium, the fluoride concentration was less than 1 ppm.

X-ray diffraction (XRD) of BG surfaces

XRD patterns demonstrate the time- and composition-dependent formation of crystalline phases on the surface of BG discs whilst in cell culture media. Diffraction patterns obtained from the 0 mol% CaF₂ group revealed an amorphous halo and lacked sharp peaks indicative of crystalline material at all time points examined (Figure 1). The 1.00 and 4.75 mol% CaF₂ groups showed no distinct peaks after 7 days, but rather produced a shift in the amorphous halo position. A single reflection at 29.5 °2θ for the 4.75 mol% group was observed after 7 days in culture indicating the formation of the calcite form of calcium carbonate (JCPDS 5-586). However, after 14 and 28 days, typical apatitic features at 26 and 32-34 °2θ were observed. All other BG groups showed peaks indicative of apatite at all the time points examined.

Scanning electron microscopy (SEM) to visualise cells and BG apatite formation

Representative SEM images of Saos-2 cells attached to BG discs show morphologically normal cells attached to the material surface (Figure 2a, b, and c). SEM images further demonstrate the presence of structures typical of apatite on BG surfaces after 7, 14 and 28 days in culture. At all time points, the 0 mol% CaF₂ group showed very few apatite-like formations (Figure 2d, e, and f). All other compositions were notable for apatite-like structures on their surfaces, as indicated by the presence of typical agglomerates of small needle-like crystals (representative images, Figure 2g-l).

Cell viability staining on BG discs

Fluorescence staining of live and dead cells on BG discs revealed remarkable differences in cell attachment, morphology and proliferation that were BG composition dependent (Figure 3). On 0 mol% CaF₂ discs, we observed limited cell attachment and proliferation. The addition of 1.00 mol% CaF₂, however, promoted increased cell proliferation, particularly at later time points, as a nearly confluent cell layer was evident after 28 days. Furthermore, after 28 days in culture, cellular aggregates were evident on compositions with 9.28 mol% CaF₂ and higher.

Total cell quantification of cells cultured with BG

Saos-2 attachment and proliferation varied depending on BG composition. After 14 days in culture, significantly more cells were attached to 1.00 mol% CaF₂ BG discs than 0, 9.28, 13.62 or 17.76 mol% CaF₂ compositions (Figure 4a). Similarly, 4.75 mol% CaF₂ discs had significantly more cells than either 9.28 or 17.76. This same trend held after 28 days in culture. Whilst cells continued to proliferate on all BG compositions, 1.00 mol% CaF₂ discs had significantly more adherent cells than any other group. The 4.75 mol% CaF₂ group also supported significantly more cells than either the 0 or 9.28 mol% CaF₂ compositions.

When the number of cells adherent to tissue culture plastic in wells containing BG discs (and thus exposed to their dissolution ions) was examined, a different trend was observed. After 14 days in culture, significantly more cells were observed in wells with 4.75 mol% CaF₂ discs when compared to all other groups at the same time point (Figure 4b). Furthermore, more cells were observed in cultures exposed to 1.00 and 9.28 mol% CaF₂ BG discs when compared to either 13.62 or 17.76. By day 28, there were significantly more cells

in wells exposed to 4.75 mol% BG than any other group. Significantly fewer cells were observed in wells exposed to the 0 mol% CaF₂ BG discs when compared to all other groups.

Alkaline phosphatase (ALP) activity in cells cultured with BG

ALP activity in Saos-2 cultured on BG discs increased with increasing BG fluoride content. After 14 days in culture, cells on 17.76 mol% CaF₂ discs produced significantly higher ALP activity per cell than those on 0 mol% CaF₂ BG discs (Figure 5a). Similarly, after 28 days in culture, cells on 13.62 and 17.76 mol% CaF₂ produced significantly higher ALP activity than those on 0 mol% discs at the same time point. In cells exposed to the dissolution products of BG discs, but not in direct contact, a similar trend was observed whereby after 14 and 28 days in culture, cells in wells containing 17.76 mol% CaF₂ BG discs had significantly higher ALP activity than all other groups at the same time point (Figure 5b). Interestingly, after 14 and 28 days in culture, cells in wells containing 1.00 mol% CaF₂ BG discs also showed increased ALP activity, which was significantly higher than that detected in 0, 4.75 or 9.28 mol% CaF₂ groups.

Interleukin-6 (IL-6) release from cells cultured with BG discs

IL-6 release from cells cultured with BG discs was higher in groups with higher BG fluoride content. Indeed, the amount of IL-6 released per cell after 7 days from Saos-2 cultured with 17.76 mol% CaF₂ was significantly greater than that detected from cells cultured with any other BG composition. After 14 days, Saos-2 cultured with both the 17.76 and 13.62 mol% CaF₂ discs released significantly more IL-6 than those cultured with 1.00 or 4.75 mol% CaF₂ BG.

Metabolic and ALP activity in NaF-treated cultures

In cultures treated with NaF, early exposure to fluoride more strongly upregulated Saos-2 metabolic and ALP activity compared to long-term or late exposure. That is, after 14 days in culture, AlamarBlue[®] activity was significantly higher in cultures treated with NaF for the first 24 hours when compared to cultures treated from days 0-7, 0-14 or 7-14 (Figure 7a). Similarly, after 28 days in culture, ALP activity per mg of protein was significantly higher in cultures treated with NaF for the first 24 hours when compared to those treated from days 0-7, 0-14, 0-28, 7-14 or 14-28 (Figure 7b).

Discussion

We analysed the effects of a series of fluoride-containing BG on human osteoblasts *in vitro*. We cultured cells directly in contact with BG, whose dynamic surface is thought to affect cell attachment and proliferation, and on tissue culture plastic in the same well as BG discs so that they were exposed to the dissolved ions released from the BG. Elemental analyses of culture media samples collected throughout revealed how BG composition affected ion release and thus the level of exposure experienced by cells.

Silicon, which comprises a large proportion of BG by both weight and molar content, is thought to affect bone mineralisation as animals fed silicon-deficient diets suffer from severe skeletal abnormalities [32]. All of the BG compositions studied here released silicon,

particularly over the first week of culture. The continued release of silicon by the 0 mol% group at later time points, however, suggests that the BG continued to dissolve over the entire 28-day period. This was confirmed by XRD and SEM analyses of BG surfaces, which demonstrated that this composition never formed a detectable apatite layer. Conversely, low silicon release in the high fluoride compositions reflects the formation of apatite on their surfaces, which is sparingly soluble, and likely prevented further dissolution and continued silicon release. Furthermore, levels of calcium lower than that in standard culture medium were measured in cultures with high fluoride-content BG after 14 and 28 days. This suggests that calcium was being removed from the medium and contributing to the formation of apatite on the BG surface. This was confirmed by XRD and SEM results which both demonstrated the formation of apatite on the surface of these compositions.

We also detected very little fluoride in culture medium at later time points, which can also be explained by the formation of apatite on the surface of BG. Fluorapatite is resistant to acid degradation and dissolution (indeed, more so than hydroxyapatite), which likely prevented further degradation of BG once an initial fluorapatite layer was formed. Whilst this may seem a disadvantage of fluoride-containing BG systems, our data with NaF-treated cultures suggest that early release of fluoride may be the most efficacious means to deliver beneficial levels of ions. Indeed, when we treated Saos-2 cultures with NaF, an initial 24-hour exposure elicited significant increases in osteoblast metabolic activity after 14 days in culture, and ALP activity after 28 days when compared to either continuous treatment or treatment at later time points. This is in keeping with previous studies which have suggested that the effects of fluoride are stronger on osteoblast precursors as opposed to more mature cells [22]. Furthermore, although the continuous delivery of therapeutic ions *via* a biomaterial may appear advantageous, excessive release can cause adverse effects. Excess fluoride can cause skeletal fluorosis, damaging bone structure and decreasing its strength. And indeed, caution should be exercised in general when substituting reportedly therapeutic ions into BG. Although zinc, for example, plays a number of essential biological roles in the body, particularly in bone formation, toxicity can result if released levels are too high [33].

Interestingly, the levels of ions detected in cell culture media after up to 28 days exposure to BG differed markedly from those observed in our previous studies in which an identical BG series was soaked in Tris buffer or simulated body fluid (SBF)[26, 34]. This suggests that the precise composition of the solutions BG are exposed to plays an important role in BG ion release and should be considered when *in vitro* studies are applied to biological systems.

The crystalline phases formed on the surfaces of the BG examined here were apatite like. They may correspond to hydroxyapatite, fluorapatite or a mixed fluorohydroxyapatite (although XRD cannot distinguish between them). Our previous examinations of these BG with ¹⁹F solid state NMR have shown that a fluoridated apatite is present in BG containing fluoride [34, 35], however, we found no indication of a fluorite crystal phase (CaF₂) for any composition at any time point examined here. This is in contrast to our previous work which demonstrated that when the same BG were incubated in SBF or Tris buffer, they formed a combination of fluorapatite and fluorite, with a greater proportion of fluorite in BG with higher fluoride contents [34, 36]. Our findings here are most likely due to the relatively high levels of phosphorus in RPMI 1640 culture medium (174 ppm) compared to SBF (31 ppm)

or Tris buffer (0ppm), which favours fluorapatite formation over fluorite. These observations also demonstrate the limitations of SBF testing, as experiments with cell culture medium, which are more regularly exchanged, may provide a more *in vivo*-like model to examine how bodily fluids will interact with BG surfaces.

Cell culture experiments demonstrated clear effects of BG composition on cell attachment, proliferation, and ALP activity. These effects were also dependent on whether the cells were in direct contact with the BG or just exposed to their dissolution ions. Total cell quantification experiments revealed that 1.00 mol% CaF₂ BG supported significantly greater numbers of cells than any other group, however, the cells proliferated as a monolayer and failed to form aggregates, often referred to as 'bone nodules'. This suggests that the formation of a surface apatite layer strongly promoted cell attachment and proliferation, but signals for differentiation, were lacking. Conversely, very few cells adhered to or proliferated on 0 mol% CaF₂ BG. The lack of crystalline peaks in the XRD pattern for the 0 mol% CaF₂ BG confirms that this composition never formed detectable amounts of an apatite-like phase on its surface. The nanocrystalline apatite formed on BG is thought to promote protein adsorption and thus aid in cell attachment [37]. In BG with higher fluoride contents, whilst cell attachment to BG surfaces was low by comparison with the 1.00 mol% CaF₂ group, cells formed dense aggregates, as were evident in fluorescence microscopy images, and had significantly higher ALP activity than those on lower fluoride content BG. Osteoblasts are known to form mineralising nodules in culture as part of the differentiation process [38]. Although we did not examine cellular aggregates for mineral formation, the presence of nodular structures and increased ALP activity suggest that either cell interactions with the apatite surface or ions released from the high fluoride-content BG promoted cell differentiation.

The effects of fluoride-containing BG on the proliferation and differentiation of cells only exposed to their dissolution ions, however, were not as straightforward. That is, whilst ALP activity per cell was highest in groups exposed to the dissolution ions of BG with the highest fluoride contents, cell proliferation was highest in the 4.75 mol% CaF₂ group. This result appears counterintuitive as fluoride has been shown to enhance osteoblast proliferation [19]. Nevertheless, calcium has also been shown to play a role in osteoblast proliferation, but with an inverse effect [39]. Calcium, which was most likely lost from solution as a result of precipitation reactions on the BG surface, was lowest in the highest fluoride BG groups, which suggests that the combination of fluoride and calcium ions in this more intermediate group promoted cell proliferation to the greatest extent. Lower proliferation in the higher fluoride-containing groups could also arise from toxicity as Bergandi *et al.* have demonstrated oxidative stress-dependent toxicity associated with osteoblast exposure to fluoride and fluoride-containing bioactive glasses [40]. Nevertheless, fluoride-mediated toxicity appears to be cell line dependent [41–43] and could arise from differences in culture techniques (particulate versus monolith bioactive glass [40]). Furthermore, studies reporting the level at which fluoride produces a cytotoxic effect are conflicting [41].

Interleukin-6 (IL-6) is a multifunctional cytokine involved in a range of pro- and anti-inflammatory processes. In bone, IL-6 is produced by osteoblasts where it acts to stimulate osteoclast differentiation and promote bone resorption [44]. Nevertheless, IL-6 levels are

reduced in post-menopausal women and significantly correlated with bone loss [45]. Furthermore, osteoporotic patients treated with PTH show elevated serum levels of IL-6 [46]. Indeed, fracture healing and bone mineralisation is delayed in IL-6 knockout mice when compared to wild-type controls [47]. Together these data suggest that whilst IL-6 promotes osteoclast activity and bone resorption, it is a marker for bone formation. Here, our data show increased IL-6 secretion per cell with increased fluoride content in the BG. This is in keeping with reports of increased IL-6 secretion from osteoblasts in patients treated with PTH [48, 49], and suggests that fluoride-containing BG may promote a similar bone formation response.

Conclusions

In summary, we have shown that fluoride-containing BG, which have the ability to release fluoride locally at an implant site, affect osteoblast cells *in vitro*, promoting osteoblast differentiation and stimulating markers for bone formation. These effects may make them good candidates for a range of bone regeneration applications.

Acknowledgements

The authors acknowledge funding from the UK Technologies Strategy Board and laboratory assistance from Ms Sabrina Skeete.

References

1. Norton MR, Wilson J. Dental implants placed in extraction sites implanted with bioactive glass: human histology and clinical outcome. *Int J Oral Maxillofac Implants*. 2002 Mar-Apr;17(2):249–57. [PubMed: 11958408]
2. Rust KR, Singleton GT, Wilson J, Antonelli PJ. Bioglass middle ear prosthesis: long-term results. *Am J Otol*. 1996 May; 17(3):371–4. [PubMed: 8817012]
3. Gentleman E, Fredholm YC, Jell G, Lotfibakhshaiesh N, O'Donnell MD, Hill RG, et al. The effects of strontium-substituted bioactive glasses on osteoblasts and osteoclasts in vitro. *Biomaterials*. 2010 May; 31(14):3949–56. [PubMed: 20170952]
4. Featherstone JD. The science and practice of caries prevention. *J Am Dent Assoc*. 2000 Jul; 131(7): 887–99. [PubMed: 10916327]
5. Lundy MW, Wergedal JE, Teubner E, Burnell J, Sherrard D, Baylink DJ. The effect of prolonged fluoride therapy for osteoporosis: bone composition and histology. *Bone*. 1989; 10(5):321–7. [PubMed: 2605048]
6. Riggs BL, Hodgson SF, O'Fallon WM, Chao EY, Wahner HW, Muhs JM, et al. Effect of fluoride treatment on the fracture rate in postmenopausal women with osteoporosis. *N Engl J Med*. 1990 Mar 22; 322(12):802–9. [PubMed: 2407957]
7. Meunier PJ, Sebert JL, Reginster JY, Briancon D, Appelboom T, Netter P, et al. Fluoride salts are no better at preventing new vertebral fractures than calcium-vitamin D in postmenopausal osteoporosis: the FAVOStudy. *Osteoporos Int*. 1998; 8(1):4–12. [PubMed: 9692071]
8. Eanes ED, Reddi AH. Effect of Fluoride on Bone-Mineral Apatite. *Metab Bone Dis Relat*. 1979; 2(1):3–10.
9. Balena R, Kleerekoper M, Foldes JA, Shih MS, Rao DS, Schober HC, et al. Effects of different regimens of sodium fluoride treatment for osteoporosis on the structure, remodeling and mineralization of bone. *Osteoporos Int*. 1998; 8(5):428–35. [PubMed: 9850350]
10. Choubisa SL. Endemic fluorosis in southern Rajasthan, India. *Fluoride*. 2001 Feb; 34(1):61–70.
11. Russell RGG. Bisphosphonates: Mode of action and pharmacology. *Pediatrics*. 2007 Mar; 119:S150–S62. [PubMed: 17332236]

12. Durie BGM, Katz M, Crowley J. Osteonecrosis of the jaw and bisphosphonates. *New England Journal of Medicine*. 2005 Jul 7; 353(1):99–100.
13. Neviaser AS, Lane JM, Lenart BA, Edobor-Osula F, Lorch DG. Low-energy femoral shaft fractures associated with alendronate use. *Journal of Orthopaedic Trauma*. 2008 May-Jun;22(5): 346–50. [PubMed: 18448990]
14. Jilka RL. Molecular and cellular mechanisms of the anabolic effect of intermittent PTH. *Bone*. 2007 Jun; 40(6):1434–46. [PubMed: 17517365]
15. Reid IR, Cundy T, Grey AB, Horne A, Clearwater J, Ames R, et al. Addition of monofluorophosphate to estrogen therapy in postmenopausal osteoporosis: a randomized controlled trial. *J Clin Endocrinol Metab*. 2007 Jul; 92(7):2446–52. [PubMed: 17440020]
16. Bellows CG, Heersche JN, Aubin JE. The effects of fluoride on osteoblast progenitors in vitro. *J Bone Miner Res*. 1990 Mar.5 Suppl 1:S101–5. [PubMed: 2339618]
17. Vestergaard P, Jorgensen NR, Schwarz P, Mosekilde L. Effects of treatment with fluoride on bone mineral density and fracture risk--a meta-analysis. *Osteoporos Int*. 2008 Mar; 19(3):257–68. [PubMed: 17701094]
18. Wergedal JE, Lau KH, Baylink DJ. Fluoride and bovine bone extract influence cell proliferation and phosphatase activities in human bone cell cultures. *Clin Orthop Relat Res*. 1988 Aug.(233): 274–82.
19. Farley JR, Wergedal JE, Baylink DJ. Fluoride directly stimulates proliferation and alkaline phosphatase activity of bone-forming cells. *Science*. 1983 Oct 21; 222(4621):330–2. [PubMed: 6623079]
20. Khokher MA, Dandona P. Fluoride stimulates [3H]thymidine incorporation and alkaline phosphatase production by human osteoblasts. *Metabolism*. 1990 Nov; 39(11):1118–21. [PubMed: 2233270]
21. Rodriguez JP, Rosselot G. Sodium fluoride induces changes on proteoglycans synthesized by avian osteoblasts in culture. *J Cell Biochem*. 2001; 83(4):607–16. [PubMed: 11746504]
22. Kassem M, Mosekilde L, Eriksen EF. Effects of fluoride on human bone cells in vitro: differences in responsiveness between stromal osteoblast precursors and mature osteoblasts. *Eur J Endocrinol*. 1994 Apr; 130(4):381–6. [PubMed: 8162169]
23. Kassem M, Mosekilde L, Eriksen EF. 1,25-dihydroxyvitamin D3 potentiates fluoride-stimulated collagen type I production in cultures of human bone marrow stromal osteoblast-like cells. *J Bone Miner Res*. 1993 Dec; 8(12):1453–8. [PubMed: 8304046]
24. Chavassieux P, Boivin G, Serre CM, Meunier PJ. Fluoride increases rat osteoblast function and population after in vivo administration but not after in vitro exposure. *Bone*. 1993 Sep-Oct;14(5): 721–5. [PubMed: 8268046]
25. Hill RG, Brauer DS. Predicting the bioactivity of glasses using the network connectivity or split network models. *J Non-Cryst Solids*. 2011 Dec; 357(24):3884–7.
26. Brauer DS, Karpukhina N, Law RV, Hill RG. Structure of fluoride-containing bioactive glasses. *Journal of Materials Chemistry*. 2009; 19(31):5629–36.
27. Brauer DS, Al-Noaman A, Hill RG, Doweidar H. Density-structure correlations in fluoride-containing bioactive glasses. *Mater Chem Phys*. 2011 Oct 17; 130(1–2):121–5.
28. Effah Kaufmann EA, Ducheyne P, Shapiro IM. Evaluation of osteoblast response to porous bioactive glass (45S5) substrates by RT-PCR analysis. *Tissue Eng*. 2000 Feb; 6(1):19–28. [PubMed: 10941197]
29. Gentleman E, Nauman EA, Dee KC, Livesay GA. Short collagen fibers provide control of contraction and permeability in fibroblast-seeded collagen gels. *Tissue Eng*. 2004 Mar-Apr;10(3–4):421–7. [PubMed: 15165459]
30. Gentleman E, Nauman EA, Livesay GA, Dee KC. Collagen composite biomaterials resist contraction while allowing development of adipocytic soft tissue in vitro. *Tissue Eng*. 2006 Jun; 12(6):1639–49. [PubMed: 16846359]
31. Allen M, Millett P, Dawes E, Rushton N. Lactate dehydrogenase activity as a rapid and sensitive test for the quantification of cell numbers in vitro. *Clin Mater*. 1994; 16(4):189–94. [PubMed: 10150166]

32. Carlisle EM. Silicon: a requirement in bone formation independent of vitamin D1. *Calcif Tissue Int.* 1981; 33(1):27–34. [PubMed: 6257332]
33. Brauer DS, Gentleman E, Farrar DF, Stevens MM, Hill RG. Benefits and drawbacks of zinc in glass ionomer bone cements. *Biomed Mater.* 2011 Aug;6(4):045007. [PubMed: 21680957]
34. Brauer DS, Karpukhina N, O'Donnell MD, Law RV, Hill RG. Fluoride-containing bioactive glasses: Effect of glass design and structure on degradation, pH and apatite formation in simulated body fluid. *Acta Biomater.* 2010 Feb 2.
35. Mneimne M, Hill RG, Bushby AJ, Brauer DS. High phosphate content significantly increases apatite formation of fluoride-containing bioactive glasses. *Acta Biomaterialia.* 2011 Apr; 7(4): 1827–34. [PubMed: 21115144]
36. Brauer DS, Mneimne M, Hill RG. Fluoride-containing bioactive glasses: Fluoride loss during melting and ion release in tris buffer solution. *J Non-Cryst Solids.* 2011 Sep 15; 357(18):3328–33.
37. Hench LL. The story of Bioglass (R). *J Mater Sci-Mater M.* 2006 Nov; 17(11):967–78. [PubMed: 17122907]
38. Bellows CG, Aubin JE, Heersche JN, Antosz ME. Mineralized bone nodules formed in vitro from enzymatically released rat calvaria cell populations. *Calcif Tissue Int.* 1986 Mar; 38(3):143–54. [PubMed: 3085892]
39. Dvorak MM, Siddiqua A, Ward DT, Carter DH, Dallas SL, Nemeth EF, et al. Physiological changes in extracellular calcium concentration directly control osteoblast function in the absence of calcitropic hormones. *Proc Natl Acad Sci U S A.* 2004 Apr 6; 101(14):5140–5. [PubMed: 15051872]
40. Bergandi L, Aina V, Garetto S, Malavasi G, Aldieri E, Laurenti E, et al. Fluoride-containing bioactive glasses inhibit pentose phosphate oxidative pathway and glucose 6-phosphate dehydrogenase activity in human osteoblasts. *Chem Biol Interact.* 2010 Feb 12; 183(3):405–15. [PubMed: 19945446]
41. Carlson JR, Suttie JW. Effects of Sodium Fluoride on Hela Cells. I. Growth Sensitivity and Adaption. *Exp Cell Res.* 1967; 45(2):415. [PubMed: 6021929]
42. Slamenova D, Gabelova A, Ruppova K. Cytotoxicity and genotoxicity testing of sodium fluoride on Chinese hamster V79 cells and human EUE cells. *Mutat Res.* 1992 May 16; 279(2):109–15. [PubMed: 1375335]
43. Yang A, Cardona DL, Barile FA. In vitro cytotoxicity testing with fluorescence-based assays in cultured human lung and dermal cells. *Cell Biol Toxicol.* 2002; 18(2):97–108. [PubMed: 12046694]
44. Ishimi Y, Miyaura C, Jin CH, Akatsu T, Abe E, Nakamura Y, et al. IL-6 is produced by osteoblasts and induces bone resorption. *J Immunol.* 1990 Nov 15; 145(10):3297–303. [PubMed: 2121824]
45. Scheidt-Nave C, Bismar H, Leidig-Bruckner G, Woitge H, Seibel MJ, Ziegler R, et al. Serum interleukin 6 is a major predictor of bone loss in women specific to the first decade past menopause. *J Clin Endocrinol Metab.* 2001 May; 86(5):2032–42. [PubMed: 11344203]
46. Buxton EC, Yao W, Lane NE. Changes in serum receptor activator of nuclear factor-kappaB ligand, osteoprotegerin, and interleukin-6 levels in patients with glucocorticoid-induced osteoporosis treated with human parathyroid hormone (1-34). *J Clin Endocrinol Metab.* 2004 Jul; 89(7):3332–6. [PubMed: 15240611]
47. Yang X, Ricciardi BF, Hernandez-Soria A, Shi Y, Pleshko Camacho N, Bostrom MP. Callus mineralization and maturation are delayed during fracture healing in interleukin-6 knockout mice. *Bone.* 2007 Dec; 41(6):928–36. [PubMed: 17921078]
48. Li NH, Ouchi Y, Okamoto Y, Masuyama A, Kaneki M, Futami A, et al. Effect of parathyroid hormone on release of interleukin 1 and interleukin 6 from cultured mouse osteoblastic cells. *Biochem Biophys Res Commun.* 1991 Aug 30; 179(1):236–42. [PubMed: 1883354]
49. Lowik CW, van der Pluijm G, Bloys H, Hoekman K, Bijvoet OL, Aarden LA, et al. Parathyroid hormone (PTH) and PTH-like protein (PLP) stimulate interleukin-6 production by osteogenic cells: a possible role of interleukin-6 in osteoclastogenesis. *Biochem Biophys Res Commun.* 1989 Aug 15; 162(3):1546–52. [PubMed: 2548501]

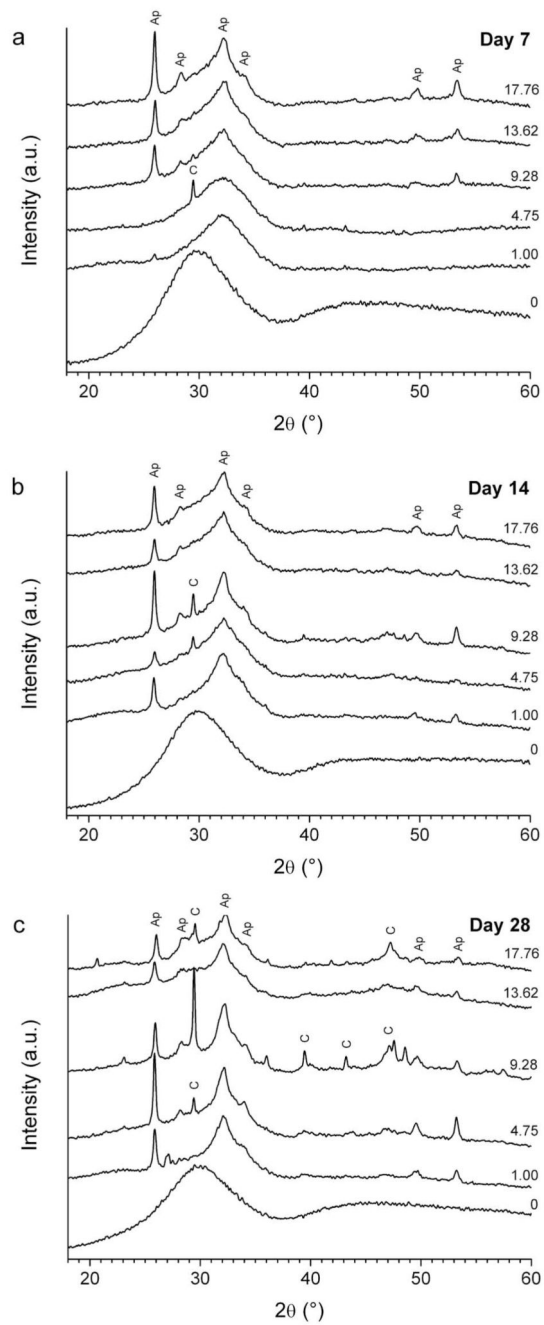


Figure 1. X-ray diffraction patterns between 18 and 60 $^{\circ}2\theta$ collected from the surface of BG discs incubated in cell culture medium for **a)** 7, **b)** 14 and **c)** 28 days. Labels indicate apatite (Ap) and calcium carbonate (C).

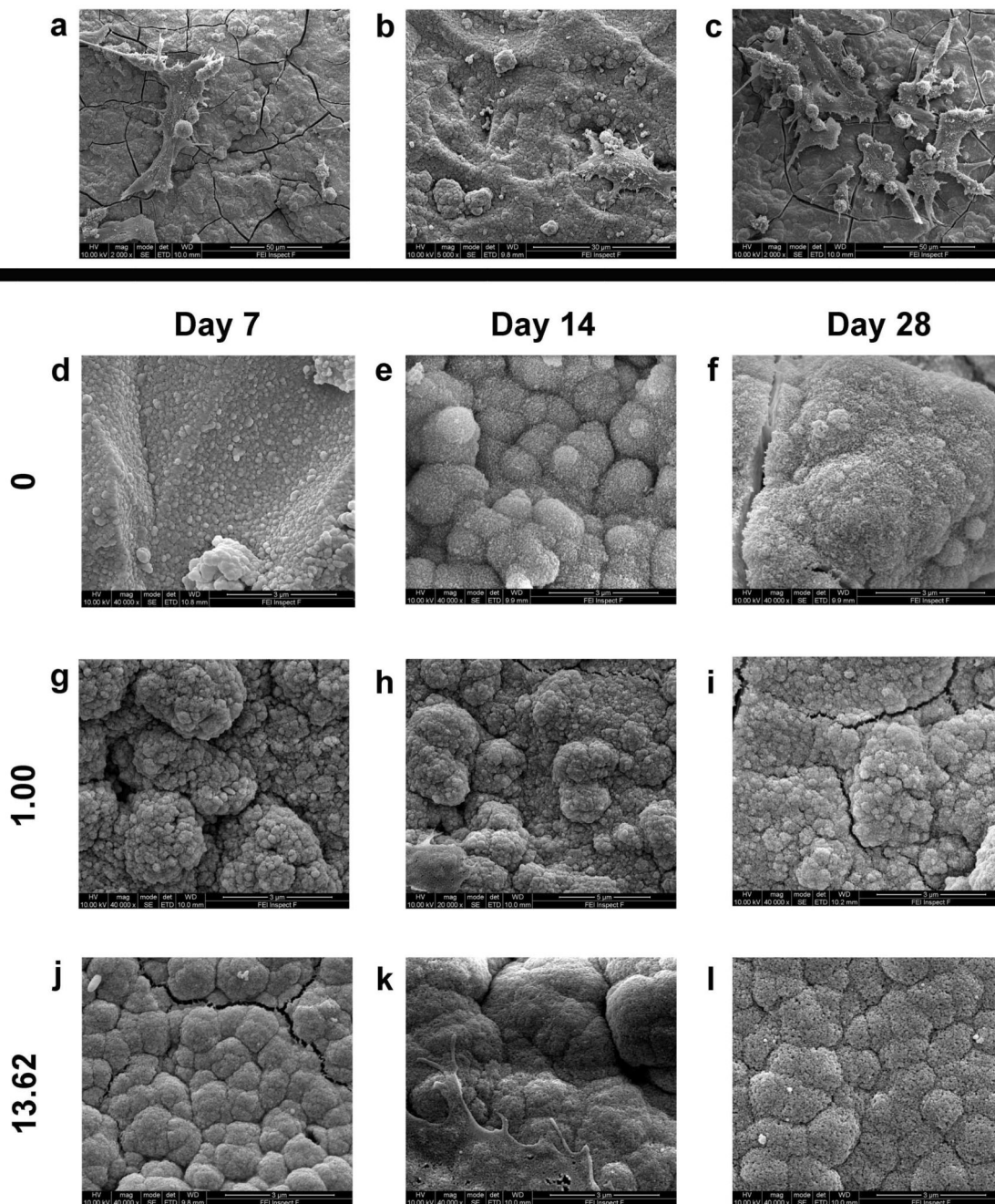


Figure 2.

Representative scanning electron microscopy images of cells adherent to BG discs containing a) 1.00, b) 9.28, and c) 17.76 mol% CaF₂ after 14 days in culture. Scale bars represent 50 μ m, 30 μ m, and 50 μ m, respectively. **d-l)** Representative images of apatite formation on BG discs of selected compositions after 7, 14 and 28 days in culture. All other groups formed apatite on their surfaces similar to that noted in the 13.62 mol% CaF₂ group. Cracks in the underlying apatite layer resulted from sample dehydration. Scale bars represent 3 μ m.

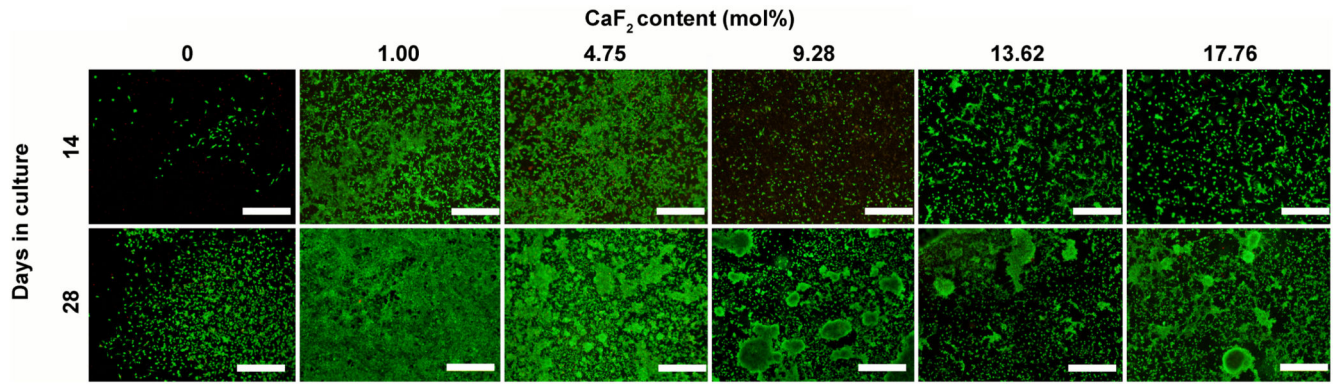


Figure 3. Cell viability staining of Saos-2 cells adherent to BG discs after 14 and 28 days in culture. Live cells appear green whilst dead cells are stained red. Scale bar = 500 μm .

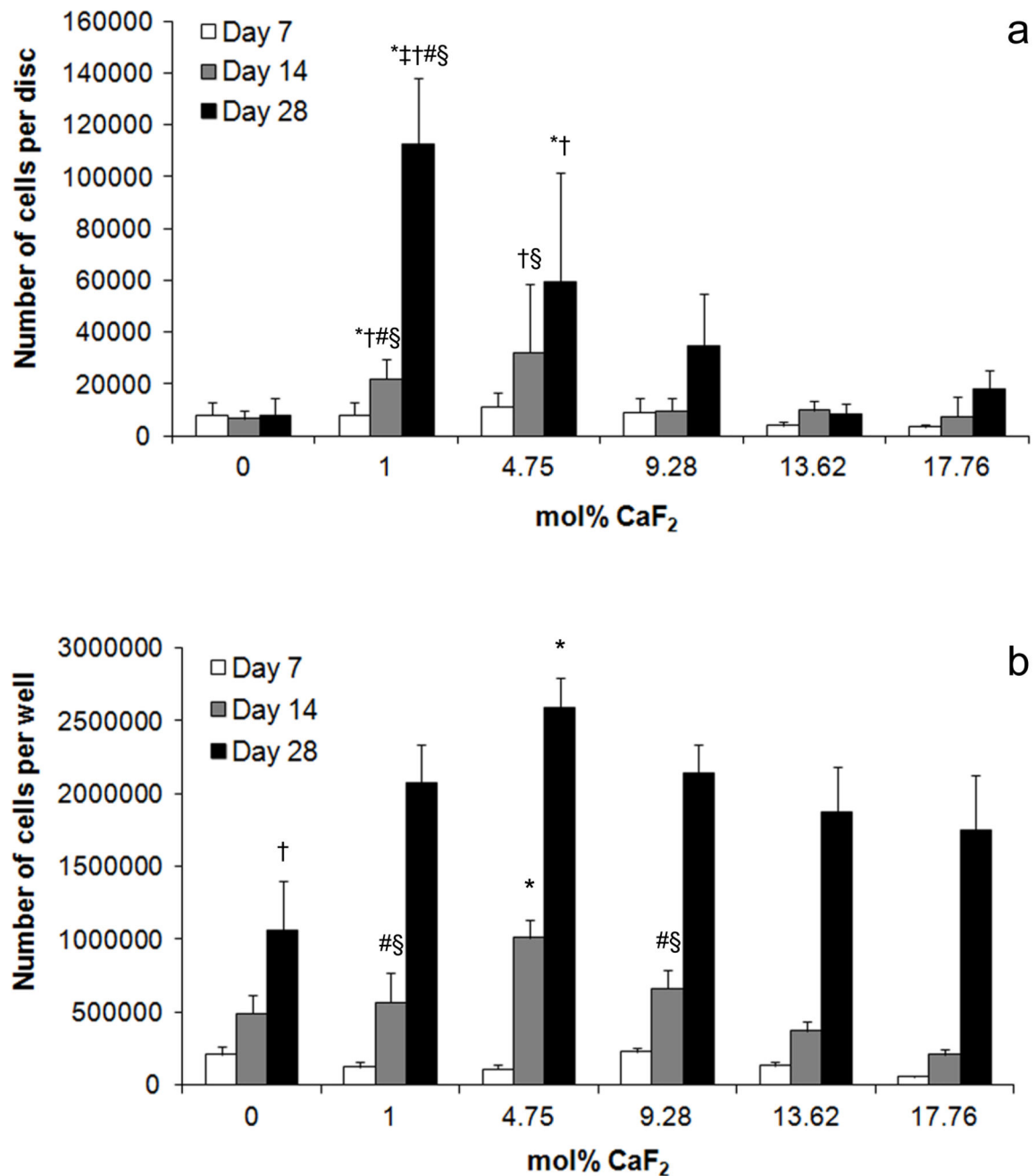


Figure 4.

a) Total number of Saos-2 adherent to BG discs after 7, 14 and 28 days in culture. * indicates significantly more cells in the indicated group compared to the 0 mol% CaF₂ group at the same time point. † significantly more cells than the 9.28 mol% CaF₂ group at the same time point. # significantly more cells than 13.62 mol% CaF₂ group at same time point. § significantly more cells than 17.76 mol% CaF₂ group at same time point. b) Total number of Saos-2 cells in cultures exposed to the dissolution products of BG discs for up to 28 days. * indicates significantly more cells in the indicated group compared to any other group at the

same time point. † significantly fewer cells than any other group at the same time point. # significantly more cells than 13.62 mol% CaF₂ group at same time point. § significantly more cells than 17.76 mol% CaF₂ group at same time point.

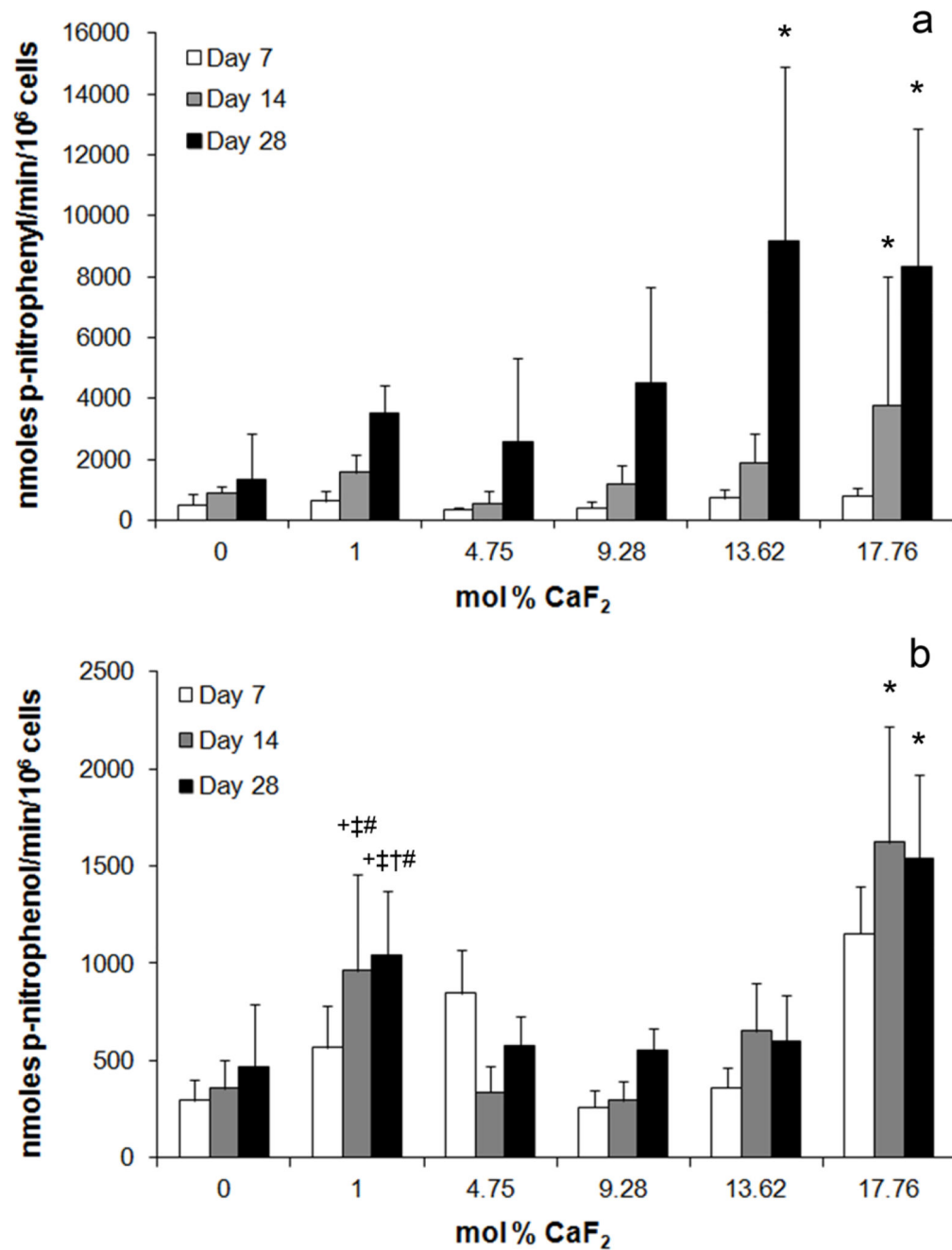


Figure 5.

a) Alkaline phosphatase activity of Saos-2 cells cultured on the surface of BG discs for 7, 14 and 28 days. * indicates significantly higher ALP activity per cell in the indicated group compared to Saos-2 on 0 mol% CaF₂ discs at the same time point. **b)** Alkaline phosphatase activity of Saos-2 cells exposed to the dissolution products of BG discs after 7, 14 and 28 days in culture. * significantly higher ALP activity compared to all other groups at the same time point. + significantly higher ALP activity than the 0 mol% CaF₂ group at same time point. ‡ significantly higher ALP activity than the 4.75 mol% CaF₂ group at same time

point. † significantly higher ALP activity than 9.28 mol% CaF₂ group at same time point. # significantly higher ALP activity than 13.62 mol% CaF₂ group at the same time point.

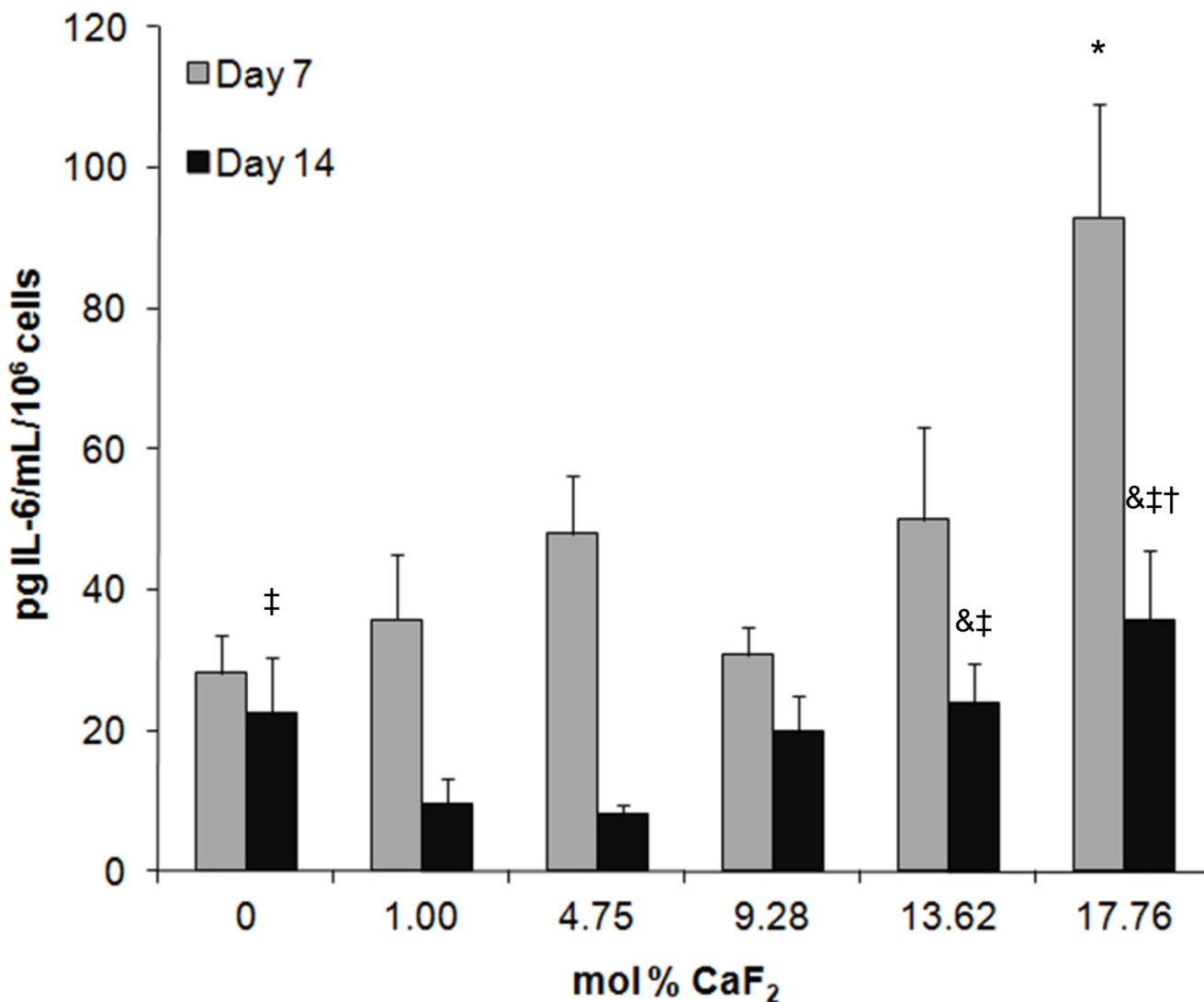


Figure 6.

Release of IL-6 from Saos-2 cultured with BG discs. * significantly higher levels of IL-6 were detected in the indicated group compared to all other groups at the same time point. & significantly higher levels compared to the 1.00 mol% CaF₂ group at the same time point; ‡ significant compared to 4.75 mol% CaF₂ group at the same time point; † significant compared to 9.28 mol% CaF₂ group at the same time point.

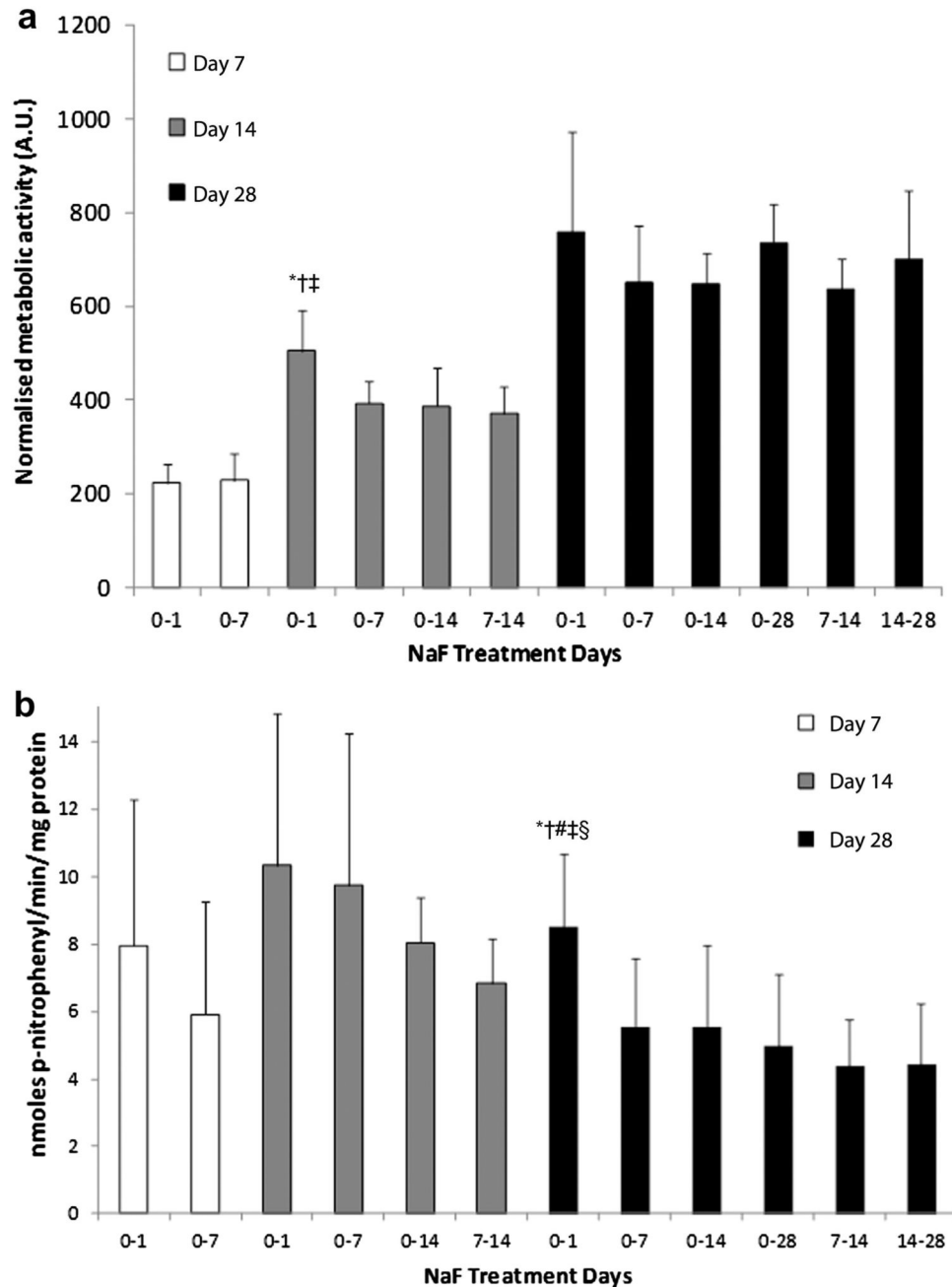


Figure 7.

a) AlamarBlue[®] activity after 7, 14 and 28 days in culture in Saos-2 treated with NaF for the indicated time periods. b) Alkaline phosphatase activity per mg protein after 7, 14 and 28 days in culture for Saos-2 treated with NaF for the indicated time periods. * significantly higher levels in the indicated group at the same time point compared to cultures treated for days 0-7. † significant compared to cultures treated for days 0-14. ‡ compared to cultures

treated for days 7-14. # compared to cultures treated for days 0-28. § compared to cultures treated for days 14-28.

Table 1

BG compositions in mole percent.

CaF₂	SiO₂	P₂O₅	CaO	Na₂O
0	49.47	1.07	23.08	26.38
1.00	48.98	1.06	22.85	26.12
4.75	47.12	1.02	21.98	25.13
9.28	44.88	0.97	20.94	23.93
13.62	42.73	0.92	19.94	22.79
17.76	40.68	0.88	18.98	21.69

Table 2

Elemental concentrations in ppm of calcium and silicon in cell culture medium over the 28 day culture period (n=3).

[Ca] (ppm)		DAY					
mol% CaF ₂		0	2	4	7	14	28
0		24.08	32.22	30.36	42.36	37.45	53.08
1		24.08	38.99	45.11	55.06	23.93	24.28
4.75		24.08	31.72	43.62	59.37	51.77	31.98
9.28		24.08	36.26	45.34	66.64	48.01	12.63
13.62		24.08	44.67	56.95	39.87	4.43	11.07
17.76		24.08	43.65	47.51	23.14	5.58	13.58
[Si] (ppm)		DAY					
mol% CaF ₂		0	2	4	7	14	28
0		0.15	22.72	23.94	27.07	35.21	50.26
1		0.15	34.45	43.92	37.67	40.21	1.53
4.75		0.15	1.52	1.08	1.38	2.97	7.67
9.28		0.15	2.05	6.74	3.31	27.13	8.06
13.62		0.15	17.85	14.72	30.33	4.32	0.23
17.76		0.15	29.94	30.06	54.36	4.87	0.52

Table 3

Fluoride concentrations in cell culture medium during pre-conditioning and over the 28 day culture period (n=3; except at days 14 and 28, n=1).

[F] (ppm)	DAY													
	Pre-conditioning													
mol% CaF ₂	-4	-3	-2	-1	1	3	5	7	14	28				
1	2.78	1.55	2.53	2.32	1.73	1.56	1.14	0.63	0.39	0.29				
4.75	5.77	1.65	1.91	1.76	1.46	0.95	0.94	0.73	0.53	0.28				
9.28	11.96	3.26	3.32	3.14	2.32	2.57	3.87	5.18	0.49	0.34				
13.62	15.86	10.66	20.01	25.97	19.92	33.76	5.90	3.04	0.64	0.27				
17.76	16.43	16.92	30.25	50.08	17.80	9.18	4.18	1.70	0.51	0.30				